MESOPOROUS ACTIVATED CARBON FIBERS FROM LIGNOCELULLOSIC MATERIALS: ADSORPTION STUDIES

S. Altenor[12], N. Passé-Coutrin[1], D. Cossement[3], J. Lambert[4], J.-J. Ehrhardt[4] and S. Gaspard[1]*
[1]*COVACHIMM, EA 3592 Université des Antilles et de la Guyane, BP 250, 97157 Pointe à Pitre Cedex. Guadeloupe*
[2]*LAQUE, Université Quisquéya d'Haïti, Port-au-Prince, Haiti*
[3]*Institut de Recherche sur l'hydrogène, Université du Québec à Trois-rivières, Québec, Canada*
[4]*Laboratoire de Chimie Physique et Microbiologie pour l'Environnement, UMR 7564 CNRS—Universite´ Henri Poincare´ Nancy 1, 405, rue de Vandoeuvre, F 54600, Villers-le`s-Nancy Cedex, France*

Abstract

High surface area and highly mesoporous activated carbon fibers (ACF) were obtained by physical activation of natural precursors (vetiver roots and bagasse) with steam and chemical activation using phosphoric acid. The textural characteristics of the activated were determined by nitrogen adsorption study and mercury porosimetry and showed that interesting porosity were obtained (S_{BET} up to 1600 m^2/g) and high mesoporous volume (V_{mes} up to 1.6 cm^3/g). A study comparing the Brunauer-Emmet-Teller (BET) and the Freundlich equation when applied to N_2 adsorption isotherm at 77 K was done. The ability of the developed activated carbons fibers to remove methylene blue and phenol from aqueous solution was investigated. Isotherm and kinetic studies were carried out to determine various factors necessary to establish adsorption treatment process. Evaluation of different isotherm and kinetic models was done to study their accuracy for modelling our adsorption data, allowing us to bring some informations on the adsorption mechanism. We also demonstrate that a recently developped fractal kinetic model could be applied to the adsorption kinetic data giving low normalized standard deviation values.

Key words: Vetiver roots - Sugarcane bagasse - activated carbon – Characterization - Adsorption.

I- Introduction

Activated carbons (ACs) are known for their great property to adsorb various molecules. They are commonly used for the treatment of gas and wastewaters or for production of drinkable water. Petroleum residues, natural coal and woods were for a long time the major AC precursors [1]. But, since a few years, others precursors at low cost and more available are used. For example, grains of sorghum [2], apricot stones [3], barks of palm tree [1], guava seeds, almond barks, hulls of dende [4], shell of coffee seeds [5], etc. are used as ACs precursors. These materials are often considered as wastes, and consequently constitute an environmental problem. As in most of the tropical countries, agricultural by-products are very abundant in the Caribbean. The reuse of those solid wastes could be important for regional economics. The preparation of activated carbon from wastes is an example of that, because high value products are obtained from low cost materials, and simultaneously brings, solutions to the problems of wastes. This would constitute not only an alternative for the more expensive precursors, but also a way to preserve the environmental quality by reducing lignocellulosic wastes accumulation and increasing the added value of these wastes materials. The present work reports the production of ACs from two natural fibrous lignocellulosic by-products, namely vetiver roots and sugarcane bagasse. These raw materials are abundant in many tropical countries, and are at low cost in comparison with synthetic precursors. Two classical methods to produce ACs were used: physical activation with steam and chemical activation with phosphoric acid. The ACs obtained were characterized in terms of their porous structure (specific surface area, pore distribution) and their adsorption ability in liquid-phase for various molecules such as phenol, methylene blue, tannic acid and gallic acid.

2- Experimental

2-1- Preparation of activated carbons

The AC were obtained from vetiver roots and sugarcane bagasse collected in Guadeloupe. These materials were initially dried at 105°C for 48 h using a drying oven and then ground. The fraction with a particle size ranging between 0,4 and 1 mm was retained for the whole of handling. Two conventional methods of preparation of AC were used: physical activation with steam under a nitrogen atmosphere at 800°C giving samples vet-H_2O and bag-H_2O and chemical activation with phosphoric acid (H_3PO_4) 85% under a nitrogen atmosphere at 600°C giving samples: vetP05, BagP05, VetP1, bagP1, VetP1.5 and BagP1.5 respectively, (P05, P1 and P1.5 are impregnation ratios; X_P (g H_3PO_4 /g precursor). For this second method, after cooling, until ambient temperature, the ACs thus obtained were washed with distilled water until stabilization of the pH, and then dried overnight using a drying oven at 105°C.

2-2- Activated carbons characterization

2-2-1- Textural characterisation

The ACs were characterized by N_2 adsorption at 77 K using a Micromeritics model ASAP-2020 analyzer. The manufacturer's software can provided BET surface area (S_{BET}) of the carbons by applying the BET equation to the adsorption data. The microporous surface (S_{micro}) and external surface (S_{ext}), the total pore volume (V_T) and micropore volume (V_{mi}) were evaluated by t-plot method, and mesopore volume (V_{me}) was estimated by Barrett-Joyner-Halenda (BJH) method [9]. The mean pore diameter, D_p, was calculated from $D_p = 4V_T/S$ [8], where V_T is the total volume of pores, and S being the BET surface area. Pore size distribution was also determined by using a mercury porosimeter, Thermo-Finnigan. Mercury porosimetry of the samples was carried out to determine meso and macro porosity, which provides a maximum operating pressure of 200 Pa.

2-2-2- Adsorption tests

Adsorption experiments with methylene blue, phenol, tannic acid and gallic acid were carried out using batch equilibration techniques. Kinetic experiments were carried out in a 250 ml glass vessel at 25°C. The recording time was started when AC was added to the vessel. At preset time intervals the concentrations were analyzed using an UV/visible spectrophotometer at 268 nm, 271 nm, 275 nm and 658 nm for gallic acid, phenol, tannic acid and methylene blue respectively. The amount of adsorption at time t, qt (mg/g), was calculated by: $q_t = V(C_0 - C_t) / W$, where, C_0 and C_t are the liquid concentrations at the start and at time t, respectively, V the volume of aqueous solution and W the mass of AC.

For adsorption equilibrium experiments, a fixed carbon concentration (40 mg) was weighted into 200 ml conical flasks containing 100 ml of different initial concentrations (50-300 mg/l and 20-100 mg/l) of methylene blue and phenol respectively. The flasks were then stoppered and agitated at 25°C until to reach equilibrium time determined by kinetics tests. After filtration, the concentrations of each solute were determined with a UV/visible spectrophotometer. The amount of adsorption at equilibrium $q_e = V(C_0 - C_e) / W$ (mg/g), was calculated, where C_e is the equilibrium liquid concentration (mg/g).

The iodine number (mg/g of AC) also was evaluated using the procedure proposed by the Standard Test Method (ASTM D 4607-86) [6,7].

3- Results and discussion

3-1- Physical properties

All the adsorption–desorption isotherms of N_2 at 77 K for activated carbons from vetiver roots and bagasse, give illustrative a mixed type in the IUPAC classification, type I at low relative pressures (P/P_0) characteristic of microporous materials and type IV at intermediate and high relative pressures characteristic of large micropores and mesopores (where a certain hysteresis slope can be observed, figure 1).

Table 1 lists physical properties of ACs including S_{BET}, S_{micro}, S_{micro}/S_{BET}, S_{meso}, V_{tot}, V_{micro}, V_{micro}/V_{tot}, V_{meso} and D_p [8]. For sugarcane bagasse ACs, increasing X_p leads to higher S_{BET} and V_{tot}, the surface area varies from 1242 m^2/g to 1502 m^2/g and the pore volume varies from 0.69 cm^3/g to 1.63 cm^3/g when Xp increases from 0.5 to 1.5. However, it is not the case for vetiver roots ACs, since the surface area and porous volume respectively increases when X_p increases from 0.5 to 1. On the other hand, when Xp increases from 1 to 1.5, the surface area value decreases from 1272 m^2/g to 1004 m^2/g as well, the total porous volume from 1.19 cm^3/g to 1.02 cm^3/g . We must also notice that the microporous fraction drops both for bag-P-1.5 and vet-P-1.5, when X_p increases. The ratio of the microporous surface to the total surface area (S_{micro}/S_{BET}) varies from 93% to 22% and 87% to 46% for bagasse and vetiver roots ACs respectively, and the the ratio of the microporous volume to the total pore volume (V_{micro}/V_{tot}) varies from 65% to 8 % and 59% to 21%, for bagasse and vetiver roots ACs respectively. This is probably due to internal etching during H_3PO_4 activation [10]. Note that, our results listed in table 1 are comparable to those reported by other works for others precursors [10] and also to certain commercial ACs [11].

Our data have been analysed using the BET isotherm, however, in two published articles [15,16] it is shown that at low pressure N_2 adsorption data of many microporous materials, can also be fitted by using either the Freundlich law $K_F P^{\alpha}$, which is the small α equation limit of a Weibull shaped isotherm, with $\alpha \leq 0.2$ or the Weibull isotherm itself. Our data were thus fitted by using the Freundlich law. For samples, BagP05, BagP1, BagP1.5, BagH_2O, Vet P05, VetP1, VetP1.5 and vetH_2O, K_F values of 409, 572.1, 520, 375, 368, 441.5, and 358 respectively are obtained. α values of 0.12, 0.138, 0.142, 0.106, 0.110, 0.138, 0.130 and 0.078 are obtained for BagP05, BagP1, BagP1-5, BagH_2O, VetP05, VetP1, VetP1-5 and vetH_2O, respectively. As previously described for microporous ACs [18,19], as well for our mesoporous AC sample, the BET surface area is also a linear function of K_F (Figure 2). Similar correlations were also obtained from an analysis of nitrogen adsorption isotherm curves published in the literature of apricot stones ACs [12], AC fibers from Nomex [13], and monolith ACs from coal [14], respectively, (data not shown). Thus, we can propose that both Brunauer, Emmett and teller expression (1) [17] and Freundlich expression (2) are equivalent:

$$n = n_m \frac{c\,p}{(p_0 - p)\left[1 + (c-1)\frac{p}{p_0}\right]} \quad (1) \qquad \text{and} \qquad n = K_F \left(\frac{p}{p_0}\right)^{\alpha} \quad (2)$$

That would be to conclude a new method for calculation of the specific surface area depending, of α and K_F by the following equation that have just to been demonstrated in a recent work [29]: $S_F = K_F S_{N2} N \frac{\alpha^{\alpha}}{(\alpha+1)^{\alpha+1}} \frac{1}{22400}$

3-2- Adsorption ability of the carbons

3-2-1- Iodine index

For AC adsorbents, the iodine index is often considered as a measure of its adsorption ability for low molar mass solutes [26]. Thus, iodine index of ACs has been calculated (table 1). As expected, the iodine index of the carbons increases with increasing the extent of Xp, and these results also show that vetiver roots provide lower iodine indexes. This results is in agreement with the nitrogen adsorption data.

3-2-2- Adsorption isotherms

The adsorption isotherm indicates how the adsorbate molecules are distributed between the liquid phase and the solid phase when the adsorption process reaches an equilibrium state. Figure 3 show the typical equilibrium adsorption of methylene blue (a) and phenol (b) on vetiver roots ACs. All curves increase steeply at low concentration, and gradually approach a plateau at high concentrations. The Langmuir and Feundlich equations are the following: $C_e/q_e = 1/bQ + C_e/Q$ *and* $\ln (q_e) = 1/n \ln (C_e) + \ln (K_F)$ [24] respectively. They are the most frequently used models to describe the experimental data of liquid phase adsorption isotherms. Both models were used to describe the relationship between the amount of phenol and methylene blue adsorbed on two ACs (vet-H2O and vetP1) and its equilibrium concentration.

a) For Langmuir model, when C_e/q_e is plotted against C_e, a straight line with a slope $1/Q$ and intercept $1/bQ$ is obtained (figure not shown), which shows that the adsorption of methylene blue and phenol on vetiver roots ACs follows Langmuir isotherm model ($R^2 = 0.999$), such as the Langmuir's parameters listed in table 2.

b) For the Freundlich isotherm Plotting $\ln (C_e)$ against $\ln (q_e)$, we can see a straight line with a slope $1/n$ and intercept $\ln (K_F)$ (not shown). The slope $1/n$ ranging between 0 and 1, is a measure of adsorption intensity or surface heterogeneity, becoming more heterogeneous as its value gets closer to zero [24]. A value of $1/n$ below 1 indicates a normal Langmuir isotherm while $1/n$ above 1 is indicative of cooperative adsorption [22]. Freundlich constants are listed in table 2. The results suggest that for both models, the adsorption of methylene blue is better than phenol. Therefore, the Langmuir isotherms fit quite well with the experimental data ($R^2 = 0.999$), whereas the low correlation coefficient ($R^2 = 0.94$ and $R^2 = 0.95$ for methylene blue and phenol respectively) shows poor agreement of Freundlich isotherm with the experimental data.

3-2-3- Adsorption kinetics

The time profiles for the adsorption of methylene blue, phenol, tannic acid and gallic acid on various carbons at 25°C are shown in figure 4. We can see the equilibrium time is reached very fast for phenol and methylene blue, below 48 h for both molecules, while for tannic acid and gallic acid, the equilibrium time go above 300 h. This could be explained on one hand by the compatibility with the size or molecular weight of these molecules and the porous structure of ACs, on the other hand by the chemical properties of ACs [10].

Several kinetic models are used to examine the controlling mechanism of adsorption process such as chemical reaction, diffusion control and mass transfer. Five kinetics models given in literature, which are pseudo-first-order, pseudo second-order, the Elovich, the intraparticle diffusion [25, 29] and the BWS *(Brouers, Weron et Sotolongo-costa)* equation [19] have been applied for the experimental data to analyze the adsorption kinetics of phenol, methylene blue, tannic acid and gallic acid.

a) The pseudo-first-order equation is expressed as: $\log(q_e - q_t) = \log q_e - \frac{k_1}{2.303}t$

Where qe and qt are amounts of dye adsorbed (mg/g) at equilibrium and time t (heure), respectively, and k_1 is the rate constant of pseudo-first-order (h^{-1}).

b) The pseudo-second-order kinetic model is expressed as: $\frac{t}{q_t} = \frac{1}{k_2 q_e^2} + \frac{1}{q_e}t$

Where k_2 is the rate constant of pseudo-second-order adsorption (g/(mg-h)) and $h = k_2 q_e^2$, where h is the initial adsorption rate (mg/g h).

c) The Elovich equation is given as follows: $q_t = \frac{1}{\beta}\ln(t + t_0) - \frac{1}{\beta}\ln t_0$

Where $t_0 = 1/\alpha\beta$. If t is much larger than t_0, the equation can be simplified as: $q_t = \frac{1}{\beta}\ln(\alpha\beta) - \frac{1}{\beta}\ln t$

d) The intraparticle diffusion is determined using the following equation: $q_t = k_{\text{int}} t^{1/2} + C$

Where C is the intercept and k_{int} is the intraparticle diffusion rate constant (mg/g $h^{-1/2}$) .

e) BWS equation is given as: $q_{n,\alpha}(t) = q_e[1 - (1 + (n-1)(t/\tau_{q,\alpha})^{\alpha})^{-1/(n-1)}]$

Where, n is the reaction order, a is a fractional time index, qe measures the maximal quantity of solute adsorbed, and a ‘‘half-reaction time’’, $\tau_{1/2}$, can be calculated, which is the time necessary to reach half of the equilibrium

The kinetics parameters of adsorption of various molecules at 25°C were calculated from the equations mentioned above and are given in table 3. The validity of the five models is checked from linear plots of *log (qe-qt) vs t, (t/qt) vs t, qt vs t ½, qt vs log (t+to)* respectively. To quantitatively compare the fitness of the model, a normalized standard deviation Δq (%) [26] and correlation coefficient (R^2) are calculated and are listed in table 3.

Firstly, values of first-order rate constant (k_1 of: 0.13 - 0.31 h^{-1} for phenol, 0.18 – 0.28 h^{-1} for methylene blue, 0.02-0.03 h^{-1} for tannic acid and 0.02 h^{-1} for gallic acid at 25°) indicate that the rate of removal is fastest for phenol and methylene blue, followed by that for tannic acid and gallic acid. The standard deviation (Δq) is very high (35% to 85%) and the correlation coefficient relatively low (R^2 ranging from 0.99 to 0.92). Moreover, the experimental q_e(exp) values do not agree with the calculated ones. This shows that the adsorption kinetic of phenol, methylene blue, tannic acid and gallic acid onto vetiver roots ACs is of the first-order. Secondly, for the pseudo second-order kinetic model, as can be seen from table 3, the correlation coefficients (R^2 = 0.98 to 0.99) and the calculated q_e values (44 to 164, 82 to 115, 269 to 333 and 204 to 285 respectively for phenol, methylene blue, tannic acid and gallic acid agree with the experimental q_e(exp) ones. These results indicates that the adsorption kinetic of all the studied molecules follows a pseudo second-order kinetic model at all time intervals.

For the Elovich equation, the best values parameters are obtained only with phenol (R^2 = 0.94 to 0.99 and Δq = 1% to 5.6%) and tannic acid (R^2 = 0.99 and Δq =1.05% to 12%), as shown in table 3. On the other hand, for the intraparticle diffusion model, the parameters values (R^2 between 0.70 to 0.98 and Δq between 4.8% to 15%) indicate a low applicability of this model for the adsorption of these molecules onto the vetiver roots ACs. Indeed, the intraparticle diffusion model plots present two linear parts (data not shown). The intraparticle diffusion is likely to occur in two stages. The first part can be attributed to the external surface adsorption stage, and the second part corresponds to the final equilibrium stage. The adsorbate molecule rapidly enters wider mesopores and mesopores and then penetrates more slowly into wider micropore [21]. This implies that the intraparticle diffusion of phenol, methylene blue, tannic

acid and gallic acid into small mesopores may be the rate-limiting step in the adsorption process. Finally, the kinetics parameters obtained with the BWS model are better. The q_e values (285 to 350, 346 to 453, 93 to 110 and 43 to 170, respectively for tannic acid, gallic acid, methylene blue and phenol) agree with the experimental q_e(exp) ones. Moreover, the correlation coefficient (R^2 = 0.98-0.99) and the low standard deviation coefficient (Δq ranging between 0.44% to 9% with two values relatively high, 24.5% for tannic acid on vet-H_2O and 33% for phenol on vetP1) prove a good applicability of this kinetic model for phenol, methylene blue, gallic acid and tannic acid adsorption on vetiver roots ACs.

4- Conclusion

The physical properties of the vetiver roots and sugarcane bagasse carbons activated by steam and H_3PO_4, as well as their characteristics for liquid-phase adsorption, were investigated. The following results are obtained:

a) For N_2 adsorption/desorption isotherms, indicates steam-activation and H_3PO_4-activation provide mesoporous activated carbons with vetiver roots and sugarcane bagasse precursors respectively. Then, the results indicate that vetiver roots and sugarcane bagasse can produce ACs with high specific surface area.

b) Irrespective of the source materials, H_3PO_4-activation produced more porosity than steam activation. Therefore, increasing of Xp leads to a widening of pores, thus increasing the mesoporous structure. In other words, H_3PO_4-activation produced a larger mean pore diameter (2.04–3.04 nm for vetiver roots and 1.9- 4.21nm for bagasse) than steam activation (2 and–2.16 nm for bagasse and vetiver roots respectively).

c) Langmuir equation best described adsorption isotherms of phenol and methylene blue on vetiver roots ACs than the Freundlich equation. The adsorption capacity of methylene blue is better than phenol in both cases as methylene blue is a larger molecule than phenol and the high mesoporous volume of our samples favour adsorption of high size molecules.

d) Among the five kinetic models used in this work, the BWS equation and pseudo second-order equation are both kinetics models implying better to adsorption of four molecules on vetiver roots ACs studied.

References

[1] Jia Guo and Aik Chong Lua, Materials Chemistry and Physics, 80, (2003), 114-119

[2] Yulu Diao, W. P. Walawender and L. T. Fan, Bioresource Technology, 81, (2002), 45-52

[3] A.M. Youssef, N.R.E. Radwan, I. Abdel-Gawad and G.A.A. Singer, Colloids and Surfaces, 252, (2004), 143-151

[4] Largitte Lucie, Thèse de doctorat de l'université Paris VI, (2000), 147 p

[5] M. C. Baquero, L. Giraldo, J. C. Moreno, F. Suárez-García, A. Martínez-Alonso and J. M. D. Tascón, Journal of Analytical and Applied Pyrolysis, 70, (2003), 779-784

[6] A. Aygün, S. Yenisoy-Karakas and I. Duman, Microporous and Mesoporous Materials, 66, (2003), 189–195

[7] A. Namane, A. Mekarzia, K. Benrachedi, N. Belhaneche-Bensemra and A. Hellal, Journal of Hazardous Materials, (2005), B119, (2005) 189–194

[8] M. A. Díaz-Díez, V. Gómez-Serrano, C. Fernández González, E. M. Cuerda-Correa and A. Macías-García, *Applied surface science*, 238, (2004), pp. 309-313

[9] E.P. Barret, P.B. Joyner and P. Halenda, *Journal of the American Chemical Society* **73** (1951), p. 373.

[10] Ru-Ling Tseng and Szu-Kung Tseng, Journal of Hazardous Materials, B136, (2006), p. 671

[11] Feng-Chin Wu, Ru-Ling Tseng and Ruey-Shin Juang, (2005), Journal of Colloid and Interface Science, 283, p. 49

[12] A.M. Youssef, N.R.E. Radwan, I. Abdel-Gawad, G.A.A. Singer, *Colloids and Surfaces A: Physicochemical and Engineering Aspects*, 252, (2005), pp. 143.

[13] F. Suárez-García , A.Martínez-Alonso, J.M.D.Tascón, *Carbon*, 42 (2004), p. 1419.

[14] L. Liu, Z. Liu, Z. Huang, Z. Liu, P. Liu, *Carbon*, 44, (2006), p. 1598.[19] [1] H. Freundlich, Colloid and Capillary Chemistry, Methuen, London, 1926.

[15] H. Freundlich, Colloid and Capillary Chemistry, Methuen, London, 1926

[16] I. Langmuir. Journal of the American Chemical Society **38** (1916), p. 2221.

[17] S. Brunauer, P.H. Emmett and E. Teller, *Journal of the American Chemical Society* **60** (1938), p. 3

[18] S. Gaspard, S. Altenor, E.A.Dawson, P.A. Barnes and A. Ouensanga, *Journal of Hazardous Materials*, doi:10.1016/j.jhazmat.2006.09.089.

[19] F. Brouers, O. Sotolongo, F. Marquez and J.P. Pirard, *Physica A: Statistical Mechanics and its Applications*, 349, (2005), p 271.

[20] Mahir Alkan, Ozkan Demirbas and Mehmet Dogan, Microporous and Mesoporous Materials, 101, (2007), 388

[21] Ewa Lorenc-Grabowska, Gra_zyna Gryglewicz, Dyes and Pigments, 74, (2007) 34-40

[22] K. Fytianosa, E. Voudriasb, E. Kokkalis, Chemosphere, 40, (2000), 3-6

[23] J.L. Figueiredo, M.F.R. Pereira, M.M.A. Freitas, J.J.M. Orfao, Carbon, 37, (1999), 1379–1389

[24] B.H. Hameed, A.L. Ahmad, K.N.A. Latiff, Dyes and Pigments,75, (2007) 143-149

[25] Yunus Onal, Journal of Hazardous Materials, B137, (2006), 1719–1728

[26] Ruey-Shin Juang, Feng-Chin Wu, Ru-Ling Tseng, Colloids and Surfaces A: Physicochemical and Engineering Aspects, 201, (2002), 191–199

[27] Ru-Ling Tseng , Feng-Chin Wu, Ruey-Shin Juang, Carbon , 41, (2003) 487–495

[28] Gaspard, S., Altenor, S., Passe-Coutrin, N., Ouensanga, A. Brouers, F., Water Research, 40, (2006) 3467-3477.

[29] N. Passe-Coutrin, S. Alténor, D. Cossement, C. Jean-Marius and S. Gaspard , (2007), subjected to Microporous and Mesoporous Materials.

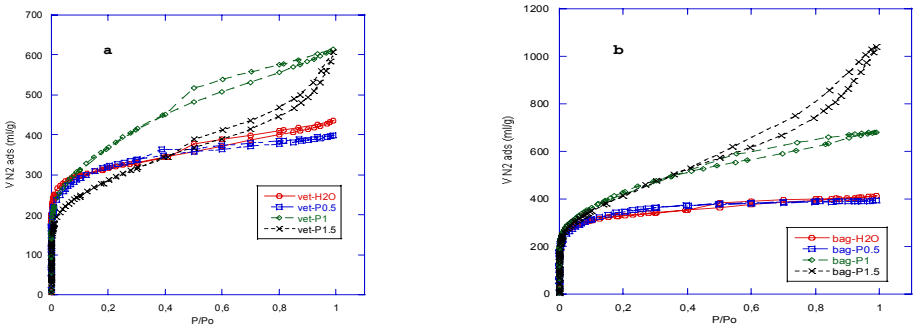

Figure 1: Adsorption/desorption isotherms of N_2 at 77 K for steam- and H_3PO_4-activated carbons derived from (a) vetiver roots and (b) bagasse

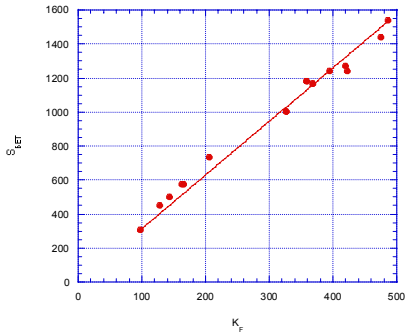

Figure 2: S_{BET} as a function of K_F, for bagasse and vetiver roots activated carbons (ACs samples from this work and from reference [28])

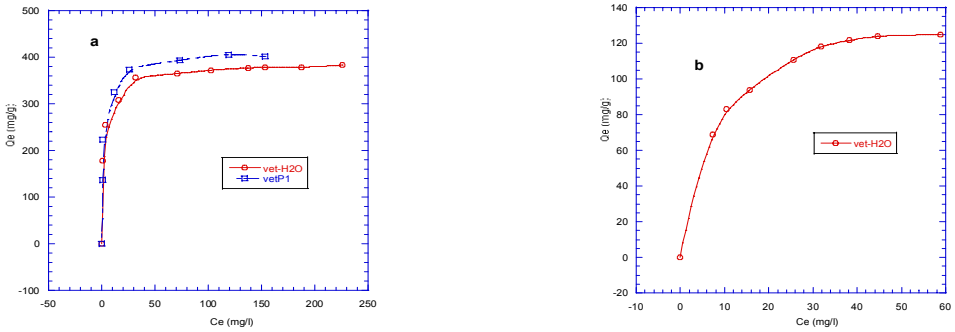

Figure 3: Equilibrium adsorption isotherms of methylene blue (a) and phenol (b) at 25°C on vetiver roots ACs

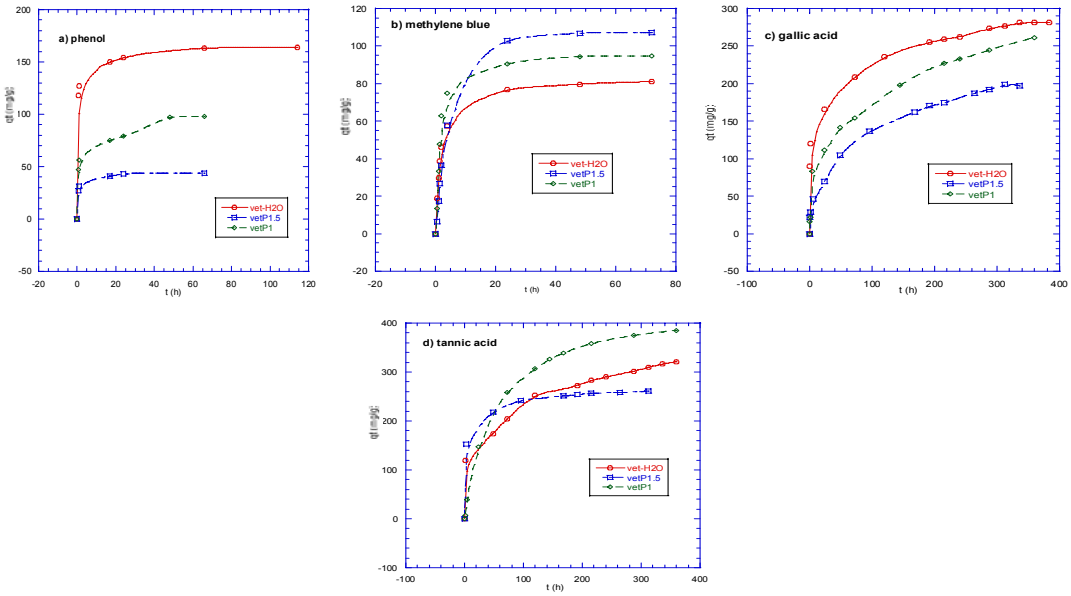

Figure 4: Experirental data and curves fits of phenol, methylene blue, gallic acid and tannic acid adsorption kinetics on vetiver roots ACs

Table 1: Physical properties of the ACs from vetiver roots and sugarcane bagasse by steam activation and chemical activation with phosphoric acid

Samples	N_2 adsorption									Hg porosimetry		iodine index
	S_{BET} (m^2/g)	S_{mi} (m^2/g)	S_{mi}/S_{BET} (%)	S_{ext} (m^2/g)	V_{mi} (cm^3/g)	V_{me} (cm^3/g)	V_{Tot} (cm^3/g)	V_{mi}/V_{tot} (%)	D_p (nm)	V_{me} (cm^3/g)	V_{tot} (cm^3/g)	(mg/g)
Vet-H_2O	1185	894	75	291	0.36	0.33	0.69	52	2.16	3.68	4.01	508
VetP0.5	1170	1017	87	153	0.45	0.31	0.76	59	2.04	0.98	1.13	668
VetP1	1272	737	58	535	0.39	0.80	1.19	33	2.83	0.98	1.11	819
VetP1.5	1004	468	46	536	0.22	0.80	1.02	21	3.04	2.13	2.19	734
Bag-H_2O	1242	1026	83	216	0.42	0.27	0.69	60	2.00	4.47	5.6	1278
BagP0.5	1269	1184	93	84	0.52	0.27	0.79	65	1.90	2.41	2.78	1285
BagP1	1502	911	60	591	0.45	0.81	1.26	35	2.8	1.76	2.09	1358
BagP1.5	1492	327	22	1165	0.14	1.49	1.63	8	4.21	2.63	2.77	1283

Table 2: Langmuir and Freundlich isotherm constants for phenol and methylene blue on vet-H_2O and vetP1 ACs at 25°C

Samples	Langmuir isotherm			Freundlich isotherm		
	Q (mg/g)	b (l/mg)	R^2	n	K_F (mg/l) $(l/mg)^{1/n}$	R^2
(phenol)						
vet-H_20	143.44	0.131	0.998	3.40	40.87	0.951
(Methylene blue)						
vet-H_20	385.16	0.37	0.9999	7.72	202.61	0.947
vetP1	407.56	0.53	0.9998	5.72	186.47	0.938

Table 3: Kinetics parameters calculated for phenol, methylene blue, tannic acid and gallic acid adsorption onto vetiver roots and sugarcane bagasse ACs

Samples	Pseudo-first order equation				Pseudo-second order equation				The Elovich equation				Intraparticle diffusion equation				BWS equation				
	q_e	K_1	R^2	Δqt(%)	q_e	K_2	R^2	Δqt(%)	α	β	R^2	Δqt(%)	K_{int}	C	R^2	Δqt(%)	qe	τ°	α	R^2	Δqt(%)
a) Phenol																					
Vét-H2O	42	0.13	0.99	85	164	0.009	0.99	19	-	0.11	0.99	1	4.5	124	0.85	4.8	170	0.19	0.18	0.99	19
VétP1	72	0.18	0.92	57	99	0.004	0.99	-	-	0.1	0.94	5.6	6.7	46	0.97	4.8	350	204	0.43	0.98	33
VétP1.5	23	0.31	0.92	69	44	0.05	0.99	7	-	0.28	0.97	3.4	2.7	28	0.82	7.8	43	0.51	0.36	0.99	0.44
b) Methylene blue																					
Vét-H2O	50	0.18	0.94	71	82	0.008	0.99	7	93	0.07	0.84	13	8.3	23	0.78	-	82.5	1.6	1	0.99	0.62
VétP1	59	0.25	0.96	66	97	0.006	0.99	-	109	0.05	0.80	-	9.7	28	0.70	-	93.4	1.4	1.59	0.99	2.06
VétP1.5	95	0.28	0.99	28	115	0.002	0.99	-	49	0.04	0.95	-	13.6	11	0.88	-	110	3.57	1.32	0.99	0.88
c) Tannic acid																					
Vét-H2O	267	0.02	0.93	35	333	0.0001	0.98	28	18	0.014	0.99	1.5	14.3	66	0.92	11	380	20.8	0.45	-	24.5
VétP1	345	0.02	0.99	39	416	$6*10^{-5}$	0.98	15	23	0.012	0.99	12	22.6	19	0.94	-	453	52.9	0.93	0.99	1.59
VétP1.5	96	0.03	0.93	71	263	0.0007	0.99	13	-	0.04	0.99	1.05	11.7	88	0.74	15	346	6.82	0.29	0.99	3.2
d) Gallic acid																					
Vét-H2O	188	0.02	0.97	54	285	0.0002	0.99	-	-	0.034	0.96	7	8.6	126	0.96	13	350	67	0.25	0.98	10
VétP1	215	0.02	0.98	56	263	0.0001	0.98	-	69	0.027	0.95	-	12.8	348	0.96	-	350	204	0.43	0.98	9.06
VétP1.5	176	0.02	0.98	46	204	0.0001	0.98	-	51	0.034	0.92	-	10	23	0.98	12	285	235	0.48	0.99	6.58